

PREDICTING THE POPULARITY OF MICRO-VIDEOS WITH MULTIMODAL VARIATIONAL ENCODER-DECODER FRAMEWORK

Yaochen Zhu, Jiayi Xie, and Zhenzhong Chen*

School of Remote Sensing and Information Engineering, Wuhan University

ABSTRACT

As an emerging type of user-generated content, micro-video drastically enriches people's entertainment experiences and social interactions. However, the popularity pattern of an individual micro-video still remains elusive among the researchers. One of the major challenges is that the potential popularity of a micro-video tends to fluctuate under the impact of various external factors, which makes it full of uncertainties. In addition, since micro-videos are mainly uploaded by individuals that lack professional techniques, multiple types of noise could exist that obscure useful information. In this paper, we propose a multimodal variational encoder-decoder (MMVED) framework for micro-video popularity prediction tasks. MMVED learns a stochastic Gaussian embedding of a micro-video that is informative to its popularity level while preserves the inherent uncertainties simultaneously. Moreover, through the optimization of a deep variational information bottleneck lower-bound (IBLBO), the learned hidden representation is shown to be maximally expressive about the popularity target while maximally compressive to the noise in micro-video features. Furthermore, the Bayesian product-of-experts principle is applied to the multimodal encoder, where the decision for information keeping or discarding is made comprehensively with all available modalities. Extensive experiments conducted on a public dataset and a dataset we collect from Xigua demonstrate the effectiveness of the proposed MMVED framework.

1 INTRODUCTION

In recent years, with the prevalence of social media, people grow increasingly enthusiastic about spreading various forms of their creations on the Internet, and the consumption of user-generated contents (UGC) has gradually become an indispensable daily entertainment activity for most of the populations. Interestingly, for tons of UGCs posted on social media every day, most of them soon fall into oblivion, while some are able to attract lots of attention and disseminate widely, reflected by receiving comparatively large amounts of views, likes, comments, reposts.

Various internal and external factors may affect the popularity of UGCs, including not only the quality of their content, the influence of their publishers, but even the release timing as well [1, 2]. Accurate predictions of the popularity level of UGC could be of great benefit: It allows the service providers to make strategic decisions as to the management of their resources, such as caching and network optimization [3], and provides users with more satisfactory personal recommendations [4]. Therefore, the popularity prediction of UGCs has received lots of attention among researchers.

Extensive work has been done in the domain of popularity prediction for traditional forms of UGCs, such as articles [1], news [5], and images [6]. Generally speaking, early studies on popularity prediction of UGC can be divided into two categories, i.e., feature-driven methods and generative (time series-driven) methods [7]. Feature-driven approaches first extracted a large number of features related to the UGC contents, the profile of users, or the social networks, and trained machine learning models such as Support Vector Machine (SVM) [6] or Random Forest (RF) [5] to optimize a mapping function from the feature

space to a pre-defined popularity space. They mainly focused on feature engineering techniques and could achieve good performance, provided that the extracted features are effective. On the other hand, for analysis of the popularity evolution pattern of UGCs over time, generative approaches utilized the temporal regularities of the popularity curve at the early stage to fit an autoregressive model with the linear or non-linear dynamics to predict its future trends [8, 9, 10]; most of them relied on strong hypotheses about the popularity accumulation mechanism. Recently, inspired by the outstanding performance of deep learning models, several deep learning-based methods for UGC popularity prediction have been proposed [7, 4] in both categories, taking advantage of the massive representative powers of convolutional neural networks (CNNs) to extract more powerful features and recurrent neural network (RNNs) to capture the more complicated temporal relationships.

However, as an emerging form of UGC, litter efforts have been dedicated to the understanding of micro-videos. Compared to popularity prediction for traditional UGCs or professionally made videos such as movies, predicting the popularity of micro-videos faces its own challenge due to the following factors: (1) **Heterogeneity**: Aside from a short video that lasts from 6 seconds to 60 seconds, several other components are usually attached, such as background music, titles, and hashtags, each describing the micro-video from a different perspective. Therefore, micro-videos are way richer in information than other forms of UGCs, which renders it more difficult to extract relevant features and fuse them effectively across modalities to explain the observed popularity trend. (2) **External Uncertainty**: Even if features that are highly informative to the popularity of micro-videos could be properly extracted and fused, since micro-videos are made to gratify the mercurial taste of the massive online audiences, the popularity of a micro-video could vary under the impacts of lots of external uncertainties such as the time of publishing, change of trends or influence from

This work was supported in part by National Key R&D Program of China under contract No. 2017YFB1002202. (Corresponding author: Zhenzhong Chen, E-mail:zzchen@iee.org)

online-celebrities and other social media. Thus, the observed popularity usually appears a certain amount of randomness. (3)

Internal Noise: Moreover, compared to the professional teams by whom the movies are made, the uploaders of micro-videos are usually unaware of various expertise such as film grammars to convey affective information to the audience[11], or lack the professional devices to shoot the video, which may lead to poor quality in both visual and acoustic contents. Besides, when users upload micro-videos online, they may make up sensational titles and tags that are irrelevant to the content just for the eye-catching effect, and the profile of users could be falsified as well, which makes the textual and user features untrustworthy.

Therefore, in order to address these challenges, we propose a multimodal variational encoder-decoder (MMVED) framework for micro-video popularity prediction. Unlike the majority of previous approaches where the map from features of a piece of UGC to its popularity level is assumed to be deterministic, MMVED learns a stochastic Gaussian embedding of a micro-video that is informative to the prediction of its future popularity level, while preserves the inherent randomness of the popularity caused by various external uncertainties simultaneously. In particular, MMVED takes the maximization of a variational approximation to the information bottleneck as its objective, such that only relevant cues in the information-rich micro-video features can be extracted into the hidden representation, ignoring the irrelevant and noisy parts. Specifically, in the multimodal encoder, we adopt the Bayesian product-of-experts strategy to fuse the modality-specific embeddings, where both the information heterogeneity and difference of uncertainty of all modalities are comprehensively considered. MMVED could also be shown to be parameter-economic to deal with the modalities missing problem in the test phase.

Please note that a preliminary conference version of this paper has been presented at WWW 2020 [12]. Compared to the initial paper that constructed the MMVED objective by adding the Variational Auto-Encoder (VAE) loss as an ad-hoc regularizer to the vanilla encoder-decoder target, this manuscript rigorously proves that such MMVED objective in essence lower-bounds the information bottleneck objective through the deep variational information bottleneck (D-VIB) theory, which further reveals the underlying information-sifting and denoising mechanism of the proposed framework; Besides, we demonstrate both theoretically and empirically that various form of decoders, such as MLP with cross-entropy loss, MLP with MSE loss or RNN could be incorporated into the MMVED framework for corresponding tasks of UGC popularity prediction, such as popularity classification, regression, and temporal regression, etc. Moreover, more advanced feature engineering techniques are utilized to characterize different aspects of the micro-video, which take advantage of recent advances of deep neural networks in both computer vision and audio processing community.

The remainder of this paper is organized as follows: Section 2 surveys related work concerning the popularity prediction task of UGCs; Section 3 expounds the proposed MMVED framework in detail; Section 4 describes the adopted feature engineering techniques; Section 5 and 6 evaluate the proposed model on two micro-video popularity prediction datasets and analyze experimental results; Finally, section 7 concludes the paper.

2 RELATED WORK

Due to its importance in recommendation, advertising, and many other applications, popularity prediction of UGCs on social media receives considerable attention in both industry and academia. The premiere step to predict the popularity of UGCs is to measure it numerically. Generally, the popularity of a piece of UGC is defined by the volume of positive response it receives, which can be estimated by the number of viewers, likes, comments, and reposts. In practice, the weighted average of any combinations of these indexes could adequately serve as an indicator of popularity levels of UGCs, and they are widely used in researches to construct the groundtruth for UGC popularity prediction tasks.

For popularity prediction of online textual contents, such as hashtags, microblogs, and articles, most studies focused on combining the representative features from the textual contents [5], [13] and the social context, such as the way users are linked, to train a popularity predictor. One exemplar work is [14], where several content features from hashtags of the tweets were fused with contextual features from the user social graph to train multiple outside classifiers. Besides, for popularity prediction of Reddit comments, Zayats and Ostendorf [15] extracted the textual features from the reviews and combined the user interaction graph with a long short term memory (LSTM) network to model the influence of user connections and temporal evolution to the popularity of comments over time.

As for predicting the popularity of images and long-videos [16] (such as those posted on YouTube) where rich information is contained in visual or aural modalities, multimodal learning that fuses information from different views is one of the most commonly used techniques. Li et al. [17] introduced a novel propagation-based popularity prediction method by considering both intrinsic video attractiveness and the underlying propagation structure. Khosla et al. [18] explored the relative significance of individual features involving multiple visual features, as well as various social context features, including the number of views and contacts. Cao et al. [19] utilized two coupled neural networks to iteratively capture the cascading effect in information diffusion to predict future popularity. Trzcinski et al. [20] predicted the popularity of the video with both the visual clues and the early popularity pattern of the video after its publish over a certain period. However, none of these methods considered the cold start scenario. In order to deal with such a challenge, McParlane et al. [6] took a content-based strategy and utilized only visual appearance and user context for Flickr image popularity prediction. Bielski et al. [4] predicted the popularity of videos before they are published, by exploiting the spatio-temporal characteristics of videos through a soft self-attention mechanism, and they intuitively interpreted the impact of contents on video popularity by Grad-CAM Algorithm.

Although an emerging form of UGC, several pioneer work have been dedicated towards the popularity prediction of micro-videos. Chen et al. [2] first employed four types of heterogeneous features, i.e., the visual, acoustic, textual, and social features to describe the characteristics of micro-videos, and proposed a transductive multimodal learning model to regress the popularity index of micro-videos after their release. Trzcinski and Przemyslaw [20], on the other hand, focused on using the early popularity pattern of the popularity curve to predict the

trend for the time after, which extended the micro-video popularity prediction task to an online manner. Afterwards, Jing et al. [21] thoroughly discussed the detrimental effects of internal noise to the micro-video analysis studies, and they augmented the multi-view learning method with a low-rank constraint, such that only a few principal patterns in micro-video features are allowed to be kept in its representation.

The most salient character that distinguishes our methods from the above ones is that we also consider the inherent uncertainty in popularity and treats all external uncertain factors as randomness, which can be properly preserved when we learn the Gaussian embedding of the micro-videos. Besides, compared with [21], which also considered the adverse effect of noise, we resort to combining the representative learning power of the deep neural network and the denoising ability of information bottleneck structure, where for each sample, the information that is allowed to be extracted into the hidden representation is actively learned and dynamically decided. Furthermore, in [21], the popularity was a single numerical value, whereas our model is also suitable for tasks where the popularity is represented by a time-related sequence, which is more difficult since it requires understanding the hidden evolutionary pattern of the popularity trend.

3 THE MULTIMODAL VARIATIONAL ENCODER-DECODER FRAMEWORK

3.1 Problem Formulation

Consider we collect a micro-video popularity prediction dataset \mathcal{D} of the form $\{(\mathbf{m}^1, \mathbf{y}^1), \dots, (\mathbf{m}^N, \mathbf{y}^N)\}$, where $\mathbf{m}^i = \{m_1^i, \dots, m_k^i\}$ is the features extracted from K modalities, and \mathbf{y}^i is the corresponding popularity groundtruth which could assume one of the following three forms: $\in \{0, 1\}$ for classification, $\in \mathbb{R}$ for regression, or $\in \mathbb{R}^T$ for temporal regression, our goal is to learn a hidden representation \mathbf{z} of a micro-video based on the integrated information from all the modalities that is highly informative for its potential popularity level, while being robust to the external uncertain factors and the internal feature noises. The main notations used in section 3 are summarized in Table 1 for the convenience of reference.

3.2 Training Objective

As the hidden representation \mathbf{z} is derived from micro-video features \mathbf{m} whereas the popularity \mathbf{y} is predicted based on \mathbf{z} , their relationship can be represented by a Bayesian chain $\mathbf{m} \rightarrow \mathbf{z} \rightarrow \mathbf{y}$ and can be modeled by an encoder-decoder framework. Since the mapping from the content of the video to its popularity may not be deterministic due to some unpredictable external factors, it is reasonable to assign \mathbf{z} some randomness, and represent both the encoder and decoder as probabilistic distributions. In this paper we assume the hidden representation \mathbf{z} lies in D -dimensional Gaussian space, and use $p(\mathbf{z}|\mathbf{m})$ and $p(\mathbf{y}|\mathbf{z})$ to denote the encoder and decoder distribution respectively.

Due to the general low quality of micro-videos, not all information from input modalities are beneficial for prediction of their popularity, and thus the noise of \mathbf{m} should not be extracted into the hidden representation. Towards this end, we first define a common criteria to measure the *relevance* level of one random

Table 1: Description of Symbols Used in Section 3

Symbol	Description
K	number of modalities in a micro-video
N	number of samples of the dataset
L	number of samples to estimate the gradient
D	dimension of the Gaussian embedding
\mathbf{m}	variable for the set of multimodal features
\mathbf{y}	variable for the popularity groundtruth
\mathbf{z}	variable for the Gaussian embedding
μ	mean of the Gaussian embedding
σ	standard deviation of the Gaussian embedding
ϕ	trainable parameters of the encoder $q(\mathbf{z} \mathbf{m})$
θ	trainable parameters of the decoder $q(\mathbf{y} \mathbf{z})$
λ	weight in the training objective
MI	mutual information operator
LLD	expected log-likelihood term of IBLBO
IBLBO	information bottleneck lower bound

variable to another, i.e. the mutual information (MI), which is formulated as follows:

$$\mathbf{MI}(\mathbf{a}, \mathbf{b}) = \mathbb{E}_{p(\mathbf{a}, \mathbf{b})} [\log p(\mathbf{a}, \mathbf{b}) - \log p(\mathbf{a})p(\mathbf{b})] \quad (1)$$

Since the learned embedding \mathbf{z} is expected to pick up only cues in the input \mathbf{m} that are *relevant* to the popularity \mathbf{y} while ignoring the noisy distractors, utilizing the MI, we can construct the following constrained optimization objective:

$$\max \mathbf{MI}(\mathbf{z}, \mathbf{y}), \text{ s.t. } \mathbf{MI}(\mathbf{m}, \mathbf{z}) \leq I_c \quad (2)$$

where I_c is maximum limit of information contained in \mathbf{z} of \mathbf{m} . The equation above forces the stochastic embedding \mathbf{z} to be expressive of \mathbf{y} while being compressive of \mathbf{m} at the same time, which provides a mechanism for the model to predict the true popularity level while accessing the minimal amount of information from the input to block the noise. By introducing a Lagrange multiplier λ , the constrained optimization problem above can be proved to be equivalent to the following unconstrained one, which has the same form as the information bottleneck first proposed in [22].

$$\max R_{IB} = \mathbf{MI}(\mathbf{z}, \mathbf{y}) - \lambda \cdot \mathbf{MI}(\mathbf{z}, \mathbf{m}) \quad (3)$$

Intuitively, λ determines the degree of penalty associated with keeping more information of \mathbf{m} in \mathbf{z} , which controls the trade-off between minimum usage of information in the input and predicting the popularity target.

Since the decoder distribution $p(\mathbf{y}|\mathbf{z})$ can take the form of any valid conditional distributions and most of which are not even differentiable, it is intractable to directly calculate the two MI terms in R_{IB} according to Eq. 1 and optimize. Therefore, we resort to the variational approach [23], which posits that the decoder comes from a tractable family of distribution \mathcal{Q} and finds a distribution $q(\mathbf{y}|\mathbf{z})$ in that family that is closest to the optimal decoder distribution measured by the KL-divergence. According to the deep variational information bottleneck (D-VIB) theory [23], for $q(\mathbf{y}|\mathbf{z})$, the R_{IB} can be proved to be lower bounded by:

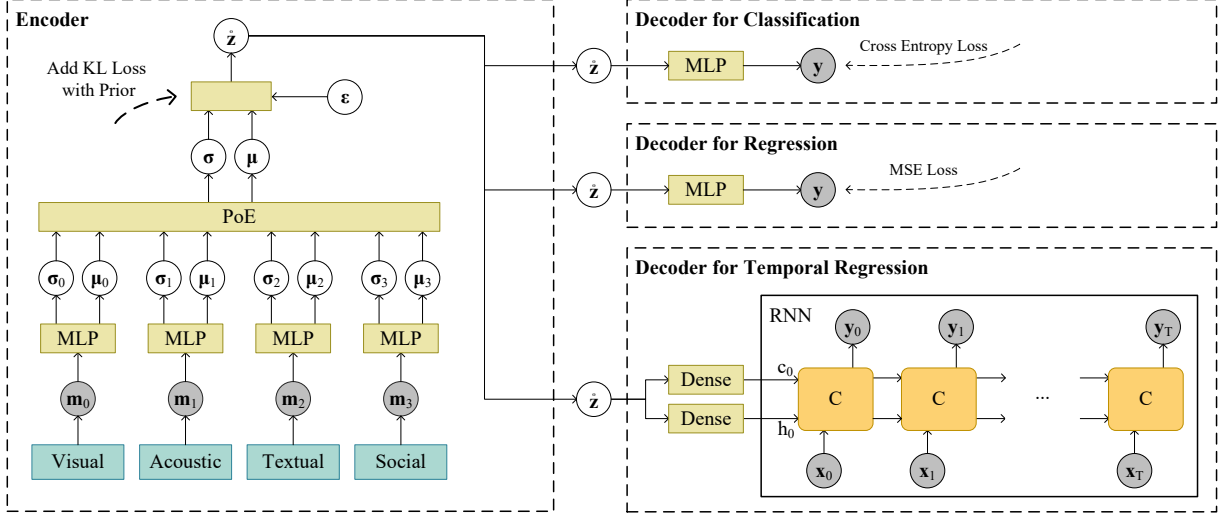


Figure 1: The framework of the proposed MMVED model for various UGC popularity prediction tasks, where the observed variables are shaded gray while the hidden ones are white. The forward steps of MMVED consist of three steps. First, features from each modality m_i of a micro-video are encoded into modality-specific hidden representations and are fused together according to the Bayesian product-of-experts principle to compute the micro-video level hidden representation \mathbf{z} , which follows $\mathcal{N}(\boldsymbol{\mu}, \boldsymbol{\sigma})$. Its KL divergence with the uninformative prior is computed as the "information bottleneck" constraint, and a λ is specified to control its "narrowness". Second, $\hat{\mathbf{z}}$ are sampled from \mathbf{z} with the reparameterization trick. Third, the popularity index of the micro-video is decoded from the $\hat{\mathbf{z}}$ through the suitable decoder.

$$\begin{aligned} \mathbf{MI}(\mathbf{z}, \mathbf{y}) - \lambda \cdot \mathbf{MI}(\mathbf{z}, \mathbf{m}) \geq \text{IBLBO} \triangleq \\ \mathbb{E}_{p(\mathbf{m}, \mathbf{y})} \left[\mathbb{E}_{p(\mathbf{z}|\mathbf{m})} [\log q(\mathbf{y}|\mathbf{z})] - \lambda \cdot \mathbf{KL}(p(\mathbf{z}|\mathbf{m}) \| p(\mathbf{z})) \right] \end{aligned} \quad (4)$$

which we note as the Information Bottleneck Lower Bound (IBLBO). The IBLBO has the same form as the OBJ we used in [12]. However, in [12], the OBJ is constructed by ad-hocly adding a VAE loss to the encoder-decoder objective. The full proof of IBLBO can be referred to in Appendix A. Hence, we can optimize IBLBO as a surrogate for the intractable R_{IB} . Note that the first expectation of Eq. 4 is taken w.r.t the data distribution $p(\mathbf{m}, \mathbf{y})$. Given that the true data distribution is usually inaccessible, the empirical data distribution is used instead, and in the rest we would omit the first expectation for simplification. The IBLBO resembles the likelihood-prior trade-off commonly found in Statistics, since the first term in the objective is the expected log-likelihood, which encourages probability density of the encoder to be put where the hidden representation could best explain the observed popularity trend, whereas the second term is the KL-divergence of the encoder distribution with the uninformative prior, which penalizes the deviation of \mathbf{z} from the prior for keeping excessive information in the input \mathbf{m} and serves as a regularizer. We name the model represented by Eq. 4 as Multimodal Variational Encoder-Decoder (MMVED) for the rest part of the paper.

3.3 The Multimodal Encoder

The stochastic encoder for the micro-video $p(\mathbf{z}|\mathbf{m})$ is parameterized as a deep neural network (DNN), more specifically, a multi-layer perceptron (MLP), which is basically a stack of fully connected layers with intermediate activations. A naive way to construct the encoder network $p(\mathbf{z}|\mathbf{m})$ is to adopt the early

fusion strategy [24], which takes the concatenated features from all modalities as its input and outputs the parameters of the encoder distribution, i.e., its mean $\boldsymbol{\mu}$ (semantic part) and logarithm of standard deviation $\boldsymbol{\sigma}$ (uncertainty and noise part):

$$[\boldsymbol{\mu}, \log \boldsymbol{\sigma}] = \text{MLP}(\text{concat}([\mathbf{m}_1, \dots, \mathbf{m}_K])) \quad (5)$$

However, such approach was shown by previous work to have unsatisfactory performance for micro-video popularity prediction task [2], since it is unable to account for the relatedness among multiple modalities. Thus, in order to make inference of \mathbf{z} based on the complementary information from all modalities, inspired by the recent advance in multimodal variational inference frameworks [25] [26], we assume conditional independence among features from each modality given the hidden embedding, i.e. $(\mathbf{m}_i \perp \mathbf{m}_j | \mathbf{z}) \quad \forall i, j < K \text{ and } i \neq j$. Then, as was shown by [25], the joint inference distribution can be factorized into the product of modality-specific encoder distributions $p(\mathbf{z}|\mathbf{m}) \propto p(\mathbf{z}) \prod_{i=1}^K p(\mathbf{z}|\mathbf{m}_i)$, which is a typical Bayesian product-of-experts (PoE) system [27]. We refer interested readers to [25] for the full prove of above deductions, and some of the most important steps are included in Appendix B for the self-containment of our paper. Such factorization means that we can first use the modality-specific encoder networks to compute the parameters of the latent representation for each modality as follows:

$$[\boldsymbol{\mu}_i, \log \boldsymbol{\sigma}_i] = \text{MLP}_i(\mathbf{m}_i), \quad i \in 1, \dots, K \quad (6)$$

Then, by using the property of multivariate Gaussian, the parameters of the hidden representation for the whole micro-video can be calculated as:

$$\begin{aligned}\mu &= \sum (\mu_i \odot (1/\sigma_i^2)) / \sum 1/\sigma_i^2 \\ \sigma &= \text{sqrt}(1/ \sum 1/\sigma_i^2)\end{aligned}\quad (7)$$

where \odot is the element-wise product operation. **Eq. 7 shows that, under the conditional independence assumption, the semantic part μ of the video-level hidden representation \mathbf{z} is in essence the average of modality-specific μ_i weighted by the reciprocal of the corresponding variance σ_i^2 . With such calculation, for experts with greater precision, which indicates that the information from their associated modalities bear less uncertainty and more relevance to the popularity prediction end, they will have more influence (larger weights) over the overall hidden representation than those with higher variance.** Another by-product of adopting such factorization is that it is easy to deal with modality missing problem in the test phase, since under such cases the only change to our framework is to remove the corresponding modality-specific encoder networks and re-compute the PoE distribution with available modalities, eliminating the needs of additional inference networks and multi-stage training regimes.

3.4 The Variational Decoders

The choice for the tractable family \mathbf{Q} of the decoder distributions $q(\mathbf{y}|\mathbf{z})$ is conditioned on the specific popularity prediction task at hand, and we will discuss three commonly faced tasks and the corresponding decoder structures.

3.4.1 Classification: MLP with Cross-entropy Loss

If the popularity groundtruth \mathbf{y} is represented as a binary variable with 1 indicating popular and 0 otherwise, the family \mathbf{Q} of the decoder distributions $q(\mathbf{y}|\mathbf{z})$ can be chosen as an MLP where the output \mathbf{o}_t is squashed through a Sigmoid function as follows:

$$q(\mathbf{y}|\mathbf{z}) = \text{Sigmoid}(\text{MLP}(\mathbf{z})) \quad (8)$$

where $\text{Sigmoid}(\mathbf{x}) = 1/(1 + e^{-\mathbf{x}})$. The maximization of the expected $\log q(\mathbf{y}|\mathbf{z})$ term in Eq. 4 is equivalent to minimization of the binary cross-entropy loss between the MLP prediction and the groundtruth.

3.4.2 Regression: MLP with MSE Loss

However, representing the popularity level of a micro-video as a binary variable is too coarse in granularity, which fails to discriminate micro-videos with different popularity degrees. Therefore, it's more common to define the \mathbf{y} as a continuous variable. Under such circumstances, in order to calculate $q(\mathbf{y}|\mathbf{z})$, we could make the following assumption:

$$q(\mathbf{y}|\mathbf{z}) \propto e^{-(\mathbf{y}-\mathbf{o})^2}, \text{ where } \mathbf{o} = \text{MLP}(\mathbf{z}) \quad (9)$$

which is equivalent to assume the output \mathbf{o} of the MLP specifies the mean of a unit-variance Gaussian distribution. Under such assumption, the $\log q(\mathbf{y}|\mathbf{z})$ term in Eq. 4 can be rewritten into the following form:

$$\log q(\mathbf{y}|\mathbf{z}) = \sum -(\mathbf{y} - \mathbf{o})^2 + C \quad (10)$$

where C is a constant, and the maximization of which is equivalent to minimizing the mean square error (MSE) loss commonly used in the regression task.

3.4.3 Temporal Regression: RNN with MSE Loss

Moreover, if the target is a popularity sequence observed at interval after the post of a micro-video, the tractable family \mathbf{Q} of the variational decoder $q(\mathbf{y}|\mathbf{z})$ can be chosen as the recurrent neural network (RNN). RNN captures the dynamic patterns of a sequence through the maintenance of a hidden state, whose value in one timestep is composed of information passed on from previous timestep and incorporation of new information from the outside. RNN is comprised of two parts: (1) a temporal dynamic that determines the internal evolution of hidden state; (2) a mapping from the RNN state to the output. Mathematically, the two parts of an RNN can be formulated as:

$$\begin{aligned}\mathbf{h}_t &= H(\mathbf{x}_t, \mathbf{h}_{t-1}) = \text{Nonlinear}(\mathbf{W}_{hh}\mathbf{h}_{t-1} + \mathbf{W}_{xh}\mathbf{x}_t) \\ \mathbf{o}_t &= O(\mathbf{h}_t) = \text{Nonlinear}(\mathbf{W}_{ho}\mathbf{h}_t)\end{aligned}\quad (11)$$

where \mathbf{W}_{xh} , \mathbf{W}_{hh} , \mathbf{W}_{ho} are the input-state, state-state, state-output transition matrices respectively. For vanilla RNN, \mathbf{z} could be directly taken as its initial state \mathbf{h}_0 . However, if long-short term memory (LSTM) [28], which addresses the exploding gradient issues of vanilla RNNs by the introduction of gating mechanism, is used, \mathbf{z} could be transformed through two distinctive dense layers to get its initial context variable and hidden state separately. The input \mathbf{x}_t at each timestep is set to be the standardized absolute time of that prediction timestep (which is different from the RNN timestep that denotes the relative time to the start) based on the observation that the popularity level of a micro-video tends to vary in a regular fashion at different times of the day. Besides, in order to avoid the error accumulation due to the exposure bias [29], predicted results from the previous timestep is not fed into the RNN cell at the next timestep as additional inputs.

Similar to the regression task, we can assume that the output of the RNN specifies the mean of a unit-variance Gaussian variable for the popularity level at each timestep:

$$q(\mathbf{y}_t|\mathbf{x}_t, \mathbf{h}_{t-1}) \propto e^{-(\mathbf{y}_t-\mathbf{o}_t)^2} \text{ where } \mathbf{o}_t = O(H(\mathbf{x}_t, \mathbf{h}_{t-1})) \quad (12)$$

Then, utilizing the local Markov assumption of the RNNs [30], i.e., $(\mathbf{o}_t \perp \mathbf{o}_{t-1}, \mathbf{h}_{t-2} | \mathbf{h}_{t-1})$, the joint probability of the whole popularity sequence \mathbf{y} can be factorized into the product of per timestep conditional probabilities (Eq. 12). Therefore, the following equation holds:

$$\log q(\mathbf{y}|\mathbf{z}) = \sum \log q(\mathbf{y}_t|\mathbf{x}_t, \mathbf{h}_{t-1}), \text{ where } \mathbf{h}_0 = \text{func}(\mathbf{z}) \quad (13)$$

Combining the Eq. 12 and 13, the $\log q(\mathbf{y}|\mathbf{z})$ can be expressed with the following form:

$$\log q(\mathbf{y}|\mathbf{z}) = \sum -(\mathbf{y}_t - \mathbf{o}_t)^2 + C \quad (14)$$

and the maximization of which is equivalent to the minimization of the sum of the per-step MSE losses.

3.4.4 Summary of the MMVED framework

By now, each component of the MMVED framework is fully specified, and we distinguish the MMVED for classification, regression, and temporal regression with MMVED-CLS, MMVED-REG, MMVED-TMP for the rest of the paper. Figure 1 schematically illustrates the structures of the proposed MMVED framework.

3.5 Monte Carlo Gradient Estimator

The above sections describe in detail each component to compute the Eq. 4. However, the optimization of Eq. 4 w.r.t the encoder $p(\mathbf{z}|\mathbf{m})$ and decoder $q(\mathbf{y}|\mathbf{z})$ is not trivial, since their gradients is in essence the gradients with probabilistic distributions, which precludes us from calculating them analytically. As a result, Monte Carlo (MC) methods are introduced to form unbiased estimators for the gradients.

We assume that the encoder and the decoder network is parameterized by ϕ and θ respectively. Since the KL term in the IBLBO can be calculated analytically, the only gradient needs to be computed by sampling is the expected log likelihood term $\text{ELL} \triangleq \mathbb{E}_{p(\mathbf{z}|\mathbf{m})} [\log q(\mathbf{y}|\mathbf{z})]$. Observing that the log $q(\mathbf{y}|\mathbf{z})$ term is explicit in expectation form, its gradient w.r.t the ELL can be easily estimated with MC by averaging the gradients computed from samples taken from the encoder distribution:

$$\nabla_{\theta} \text{ELL} \simeq \frac{1}{L} \sum_{l=1}^L \nabla_{\theta} (\log q_{\theta}(\mathbf{y}|\mathbf{z}^{(l)})) \quad (15)$$

where \simeq symbol means that the RHS is an unbiased estimator for the LHS, and $\mathbf{z}^{(l)}$ is the l th sample draw from the encoder distribution $p(\mathbf{z}|\mathbf{m})$. The unbiased estimator for the gradients w.r.t ϕ is more difficult to obtain since there is no obvious way to explicitly reform it into an expectation form. However, with reparameterization trick [31], samples from $p(\mathbf{z}|\mathbf{m})$ can be reformed by a bivariate transformation from a deterministic part and a stochastic noise of the following form:

$$\mathbf{z}([\mu, \sigma], \hat{\epsilon}) = \mu + \sigma \odot \hat{\epsilon} \quad (16)$$

where $\hat{\epsilon}$ is a random vector the same size as \mathbf{z} drawn from the standard normal distribution. Eq. 16 means that the gradients of ELL w.r.t ϕ can be estimated by drawing samples from the noise distribution taking and average:

$$\nabla_{\phi} \text{ELL} \simeq \frac{1}{L} \sum_{l=1}^L \nabla_{\mathbf{z}^{(l)}} \text{ELL} \cdot \nabla_{[\mu, \sigma]} \mathbf{z}^{(l)}([\mu, \sigma], \hat{\epsilon}^{(l)}) \cdot \nabla_{\phi} [\mu, \sigma] \quad (17)$$

As was discussed in [32], the variance of the reparameterization trick is low enough such that one sample is enough for the training to converge. Thus, the L in both Eq. 17 and Eq. 15 is set to one. **Eq. 16 can be viewed alternatively from the denoising perspective. It shows that during training, the hidden representations are injected with self-adaptive random Gaussian noises controlled by the standard deviation σ , which was shown by previous work to have robustness towards noise in the test phase compared to adding a deterministic noise in**

feature space [33], and provides a systematic way to model the latent noise generation mechanism incurred by the low-quality of micro-videos. The specific training steps of our proposed MMVED is summarized in Algorithm 1.

Algorithm 1 MMVED-SGD: Training MMVED with SGD.

Input: A micro-video popularity prediction dataset \mathcal{D} ; each sample is associated with K modalities \mathbf{m} , and the corresponding popularity representation \mathbf{y} .

- 1: Select proper decoder structure according to the task.
- 2: Randomly initialize θ, ϕ .
- 3: **while** not converge **do**
- 4: Randomly sample a batch $\hat{\mathcal{D}}$ from \mathcal{D} .
- 5: **for** $i = 1 \rightarrow K$ **do**
- 6: Compute μ_i, σ_i as Eq. 6.
- 7: **end for**
- 8: Compute μ, σ of $p(\mathbf{z}|\mathbf{m})$ from each μ_i, σ_i as Eq. 7, and add its KL-divergence with prior to the loss.
- 9: Sample ϵ from \mathbf{z} and compute z with reparameterization trick as Eq. 16.
- 10: Compute the $q(\mathbf{y}|\mathbf{z})$ as Eq. 13, and add prediction loss.
- 11: Compute gradient of loss w.r.t θ, ϕ with Eq. 15, 17.
- 12: Update θ, ϕ
- 13: **end while**
- 14: **return** θ, ϕ

Output: MMVED model trained on dataset \mathcal{D}

3.6 Predictive Behaviors of MMVED

Although MMVED appears a certain amount of randomness to deal with the interference of uncertainty in popularity during the training phase, its behavior in validation and prediction is designed to be deterministic, such that the results of different rounds of prediction for the same micro-video are consistent. Since the mean of the Gaussian variable carries the information whereas the standard deviation preserves the uncertainty, after the training of MMVED, for predicting the popularity of a newly released micro-video, the mean of the Gaussian embedding is kept as its fixed representation. Then, the extracted representation is fed into the decoder to make the prediction of the popularity.

4 FEATURE ENGINEERING

In this section, we discuss the form of \mathbf{m} , i.e., the multimodal representation of the micro-video. Previous work has confirmed that whether a micro-video comes into fashion after its release is closely related to its visual-aural contents, its attached descriptions, and the profile of its publisher [2]. Thus, features are extracted from four different aspects, namely, visual, acoustic, textual, and social, as the multimodal characterization of the micro-video.

4.1 Visual Modality

In order to describe the visual contents of the micro-video, we utilize the state-of-the-art convolutional neural network (CNN). Specifically, we keep the convolutional base of the ResNet50 [34] pre-trained on ImageNet [35] as the fixed feature extractor,

which has achieved great success in various computer vision tasks such as image classification, object detection, and action recognition.

As is shown in [36], the last layers of CNNs pre-trained on ImageNet encode the information with regard to the existence of certain objects and their relationships, which we believe could be of benefit to the popularity prediction of micro-videos, since certain objects, such as delicious food and cute pets are naturally more attractive than others. The detailed feature extraction steps are described as follows: for each micro-video, we first extract its keyframes with the FFmpeg toolkit³. Then, for each keyframe, a 2,048-D activation is obtained from the global average pooling layer of the pre-trained ResNet. In the end, the extracted activations are temporally averaged to get a fixed-length representation for the whole micro-video.

4.2 Acoustic Modality

The audio modality of a micro-video usually includes two key types of information that could be helpful to predict its popularity: the original audio track that provides complementary information with the visual elements, such as the tone and speech of the protagonists, and the accompanied background music, which shows a strong hint for the affective states of the uploader. Similarly, we use the latest CNN that is specifically designed for audio spectrogram to extract the aural features, which has shown promising results in micro-video recommendation [37], hashtag recommendation [38] and video affective content analysis [26].

In particular, for each micro-video with N_v keyframes, we first split the audio track of length N_a into N_v non-overlapping one-second windows, with the center of the i th audio window i_a computed as follows:

$$i_a = \frac{N_a - invSR}{N_v}i + 0.5invSR \quad (18)$$

where $invSR$ is the inverse of the audio sample rate. Under such cases, the center of each audio window precisely matches the position of the corresponding keyframe. Then, the spectrogram for each audio window is computed with code open-sourced by [39], and is fed into VGGish [39] pre-trained on AudioSet [40] to extract a 128-dimensional deep feature. The features for the same micro-video are globally pooled, such that video-level aural features are obtained.

4.3 Textual Modality

Besides, micro-videos are usually accompanied with textual descriptions, such as the titles, remarks, or some hashtags, to summarize the important content and emotional feelings the uploaders wish to convey, or accentuate the salient characteristics of the micro-video. Thus, the attached texts provide new aspects to support the popularity prediction. For example, a title containing "funny moments of Husky!" suggests that the micro-video is intended to resonate with a large population of pet lovers, whereas the hashtags like "AdvancedTheoryDiscovery" indicate the post videos are specially made for a small group.

³<http://ffmpeg.org/>.

For the majority of the languages that are used worldwide, mature natural language processing (NLP) toolkits are usually developed and made public by the NLP specialists. For example, the FudanNLP⁴ [41] toolkit, which is one of the most commonly referred arsenal for Chinese natural language processing, can make classification of all the texts based on models pre-trained on large corpora, and extract a 20-D textual feature vector for each sentence. As for English, the sentence2vec⁵ [42] is able to embed English sentences of variable-length into a hidden space based on their semantic similarities. Besides, the Stanford CoreNLP toolkits⁶ [43] is equipped with a broad range of text analysis packages, one of which is able to classify the input texts into five sentiment classes with pre-trained sentiment TreeBank model [44]. Both toolkits were shown to be handy for extracting reliable textual features that can support the popularity prediction of the micro-video [2, 21].

4.4 Social Modality

In addition to the features that are directly linked to the micro-video content, the profile of its publisher could also provide key information for predicting its potential popularity. For instance, uploaders who have more followers or have their accounts verified may have more influence, and their productions tend to attract more attention among viewers, in comparison with the common users.

As different micro-video sharing platforms unveil different attributes of the uploaders to the public, features from the social modality may vary from platform to platform. Nonetheless, we summarize some useful and universal social characteristics specific to the publisher: the follower-followee counts, the total post counts, the loop counts, the verification status, etc., which mainly portray the degree of influence of the uploader.

4.5 Postprocessing

Finally, all features extracted in four modalities are standardized into zero-mean and unit variance to eliminate the scale bias and stabilize the training of MMVED network.

5 EXPERIMENTS ON THE PUBLIC NUS DATASETS

5.1 Dataset and Implementation Details

We first focus on the micro-video popularity regression task with MMVED-REG model on NUS dataset. The NUS micro-video popularity regression dataset⁷ is established and released by researchers from the Lab for Media Search (LMS) at the National University of Singapore. The dataset contains 303,242 micro-videos collected between July 2015 and October 2015 from a then widely-used micro-video sharing platform Vine⁸, most of which last 6-8 seconds. The stabilized value of the comments, reposts, likes, and loops number, are recorded and averaged to formulate the sole popularity score of a micro-video. Unfortunately, at the time of our experiments, a proportion of the

⁴<https://github.com/FudanNLP/nlp-beginner/>.

⁵<https://github.com/klb3713/sentence2vec/>.

⁶<http://stanfordnlp.github.io/CoreNLP/>.

⁷<http://acmmm2016.wixsite.com/micro-videos/>.

⁸<https://vine.co/>.

links to micro-videos in the NUS dataset were invalid, and we could successfully download only 186,637 of them. Therefore, for a fair comparison, we keep the same number of test samples with previous papers (303,24, 10% of 303,242) [2, 21], and put aside another 303,24 samples for validation. The models are tested over five random splits of the dataset, and the averaged prediction performances are reported.

In our implementation of MMVED-REG model, for visual, acoustic, textual, and social modality, the number of units for the hidden layers of the modality-specific MLP encoder is empirically set to 32, 8+8 (for mean and logstd respectively). We use Adam [45] as the SGD optimizer, with learning rate initialized at $5e^{-4}$ and linearly dropped to $5e^{-5}$ at the end. Training stops after 50 epochs. As the regularization coefficient λ is very important to the performance of our framework, we will first discuss its impact in section 5.2.2, and then set it fixed to the optimal empirical value based on the experimental results in sections after.

5.2 Model Evaluation

5.2.1 Evaluation Metric

For our method to be comparable with previous work, we follow the usage of normalized mean squared error (nMSE) first proposed in [46] to measure the performance of our model. The nMSE metric is defined as follows:

$$\text{nMSE} = \frac{1}{N\sigma^2} \sum_{i=1}^N (y_i - \hat{y}_i)^2 \quad (19)$$

where y_i and $\hat{y}_i \in \mathbb{R}$ are the real and predicted popularity score for the i th micro-video sample, and σ is the standard deviation of the popularity groundtruth. Intuitively, the nMSE re-scales the normal MSE metric with the groundtruth variation, which eliminates the bias incurred by varied groundtruth variance for different dataset splits.

5.2.2 Parameter Analysis

As is aforementioned, the role λ plays can be viewed from two aspects: First, Eq. 3 shows that λ controls the penalty for encoding extra unit of information of the input modalities \mathbf{m} into the hidden representation \mathbf{z} ; Second, Eq. 4 shows that λ is the weight for the KL term and thus controls the penalty for deviation of the encoder distribution from the standard Gaussian prior. Both views can be unified in the sense that the closer the encoder distribution is to the uninformative prior, the less information in \mathbf{m} would be left in \mathbf{z} .

In order to find the optimal value for λ , we train our MMVED-REG with different settings of λ , record their training dynamics, and evaluate their performance on the test set. The results are illustrated in Figure 2. As we can find out from Figure 2, generally, the test performance increases first and then drops with the increment of λ . Such phenomenon could be explained by the fact that when the value of λ is too small, the information bottleneck constraint set on the Gaussian representation is relaxed, and thus information flows unbridledly from the noisy input modalities to the hidden representations, which makes the training unstable, oscillating and hard to converge (the blue curve). On the other

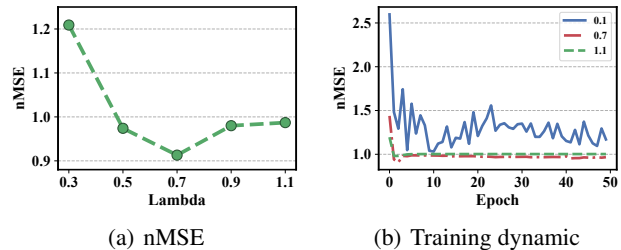


Figure 2: The influence of λ to model performance and training dynamic

hand, when the value of λ grows too large, excessive constraint is set upon the hidden embedding, where useful information for popularity prediction is blocked out as well as the noisy ones; therefore, the multimodal encoder is unable to learn a good representation from the micro-video content, which leads the model to converge to a suboptima (the red curve) compared to the model trained with a suitable λ (the green curve).

Besides, we notice an interesting phenomenon that for our model, making insufficient information constraint ($\lambda = 0.1$) is worse than imposing oversized information constraint ($\lambda = 1.1$). Such results could reveal that the information-rich but low-quality nature of micro-videos renders the extracted multimodal features low in signal-to-noise ratio, which not only interferes with but sabotages the training process and generalization ability of the popularity prediction model. Therefore, based on the analysis above, we fix λ of the MMVED-REG to its empirical optimal value 0.7, when we draw the comparison with other SoTA methods on the NUS dataset in the next section.

5.2.3 Comparison with the State-of-the-Arts

The SoTA methods that are selected for the comparison with the proposed MMVED-REG model are listed below:

- **ELM**. The extreme learning machine [47], [48] is a widely used regression model that is comprised of a single hidden layer neural network. The ELM is shown to be able to learn the embedding of various types of feature while having high generalization and low computational costs.
- **TMALL**. The transductive multi-modal learning model [2] regresses the popularity of micro-videos through learning embeddings of micro-videos where the hidden space is constrained to be consistent with the multimodal feature spaces, such that the semantic characteristics of micro-videos are preserved.
- **TRLMVR**. The transductive low-rank multi-view regression model [21] is an extension of TMALL, where a novel low-rank constraint is set upon the learned micro-video embeddings such that only principal components of the feature space are allowed to be kept in the representations.

Table 2 reports the performances of the proposed MMVED-REG and the SoTA algorithms. From Table 2, we first notice that compared to ELM where features from different modalities are

Table 2: Comparison of performance between the proposed MMVED-REG model and several SoTA methods.

Methods	nMSE
ELM [48]	0.982
TMALL [2]	0.979
TRLMVR [21]	0.934
The proposed MMVED-REG	0.914

The best results are in **bold**.

simply concatenated, TMALL utilizes a multi-view method to fuse heterogeneous features from four modalities subject to a consistency constraint, and it achieves a better result than ELM. TRLMVR further improves TMALL by adding a low-rank constraint of hidden space to the multi-view learning objective such that the insignificant components of the feature spaces are removed, which leads to substantial improvements compared to TMALL. However, in TRLMVR, the low-rank constraint is hardwired and universal for all samples, such that samples with different noise levels could not be properly distinguished. Besides, their hidden representation of TRLMVR is inherently deterministic. On the other hand, in our MMVED-REG model, we first preserve the uncertainty of popularity mapping by modeling the hidden representation as a Gaussian variable. In addition, for each micro-video, the mean (semantic part) and std (uncertainty and noise part) of its Gaussian embedding are independently inferred through the PoE inference network. Furthermore, an information bottleneck constraint is set upon the Gaussian embeddings, such that the relevant information obscured by the information-rich but noisy micro-video contents can be actively learned to be extracted into the hidden representation with the guidance of the training popularity groundtruth. Therefore, our method achieves the best results among the SoTA methods.

6 EXPERIMENTS ON CRAWLED XIGUA DATASET

6.1 Dataset and Implementation Details

Next, our discussion shifts towards the temporal popularity prediction of micro-videos on Xigua dataset. The Xigua micro-video dataset is established based on a famous micro-video sharing platform Xigua⁹ in China, whose distinguishing characteristic is that the increments of loops for each micro-video are contiguously recorded every 15 minutes immediately after its release for 3 days, which makes the popularity groundtruth a sequence. The detailed crawling strategy and dataset description can be referred to in [12]. Xigua dataset includes 3,231,072 records from 11,219 micro-videos posted by 2664 users between July 24th and August 14th, 2019. In Xigua dataset, the ResNet visual feature is reduced to 128D by PCA to prevent overfitting, and the followers/followees counts of the uploader together with the verification status are recorded as the 3D social feature.

Since predicting popularity every 15-minute is too fine in granularity for practical use, the popularity sequences are re-sampled such that the recording interval T_{int} is equivalent to 8 hours for the main part of the experiments. Nonetheless, the influence of T_{int} will be thoroughly discussed in section 6.2.4. The

⁹<https://www.ixigua.com/>

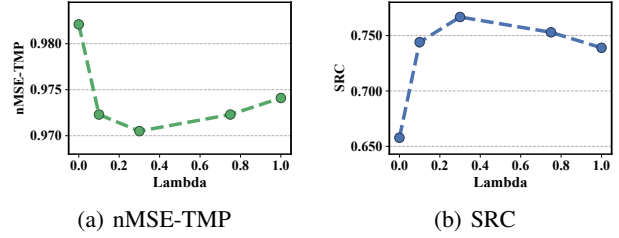


Figure 3: Influence of λ to performance of proposed MMVED-TMP model under the nMSE and SRC metrics.

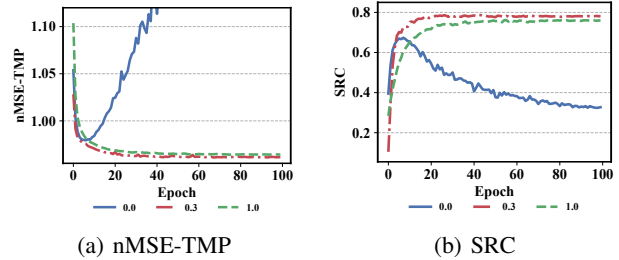


Figure 4: Influence of λ to training dynamics of proposed MMVED-TMP model under the nMSE and SRC metrics.

reported performances, unless other-wisely specified, are the averaged results over five splits, each of which randomly selects 64% of the micro-videos for training, 16% for validation, and 20% for testing. For the implementation of MMVED-TMP, the encoder structure, and the training strategy remain similar to MMVED-REG. Besides, the dimension of the hidden units for the variational RNN decoder is set to 8 empirically.

6.2 Model Evaluation

6.2.1 Evaluation Metrics

Two metrics are utilized in our work to evaluate the performance of different temporal popularity prediction methods. The first is the temporal normalized Mean Squared Error (nMSE-TMP), which is a variant of nMSE that is suitable for the measure of closeness between two sequences. The nMSE-TMP metric utilized in our paper is defined as:

$$\text{nMSE-TMP} = \frac{1}{N\sigma_y^2} \sum_{i=1}^N \frac{1}{T} \sum_{j=1}^T (\mathbf{y}_i^j - \hat{\mathbf{y}}_i^j) \quad (20)$$

where \mathbf{y}_i and $\hat{\mathbf{y}}_i \in \mathbb{R}^T$ are the real and predicted popularity sequence for the i th micro-video sample in the dataset, and σ stands for the standard deviation operator. The nMSE-TMP index rescales the mean squared error of predictions by the groundtruth variance, which alleviates the bias due to the difference of fluctuation among popularity sequences and the difference of variation among the dataset splits.

Besides, observing that even two sequences close enough measured by the nMSE-TMP could have the opposite trend, we adopt the Spearman's rank correlation (SRC) metric [18] as a complement, which is defined as follows:

$$\text{SRC} = \frac{1}{N} \sum_{i=1}^N \frac{1}{T} \sum_{j=1}^T \left(\frac{\mathbf{y}_i^j - \bar{\mathbf{y}}_i}{\sigma_{\mathbf{y}_i}} \right) \left(\frac{\hat{\mathbf{y}}_i^j - \bar{\hat{\mathbf{y}}}_i}{\sigma_{\hat{\mathbf{y}}_i}} \right) \quad (21)$$

Generally, SRC indicates the trend consistency of the prediction, which is complementary to the nMSE-TMP metric since the latter one only focuses on the deviation of squared absolute value between \mathbf{y}_i and $\hat{\mathbf{y}}_i$.

6.2.2 Parameter Analysis

Similarly, we first analyze the impact of λ to the performance and training dynamic of MMVED-TMP model under the nMSE and SRC metric. The results are illustrated in Figure 3 and 4. From both figures, we can find out that the relationship between λ , model performance, and training dynamic is in line with the regression task. Both metrics indicate that the model performance improves first but then worsens with the increment of λ . Besides, with λ set to 0, where no information constraint is set upon the hidden representation, the validation performance slightly increases in the first few epochs but drops drastically afterwards, which indicates that the model overfits to the noise and irrelevant information specific to the training set, whereas with λ set to 0.3 or 1, since the information capacity of the embedding is restricted by the KL divergence constraint, the validation performance improves in a nearly monotonic manner. Moreover, with the λ set to the suitable value ($\lambda = 0.3$), the asymptotic optimal performance of MMVED-TMP is better than those with too large λ .

Besides, we also note several differences between MMVED-TMP on the Xigua dataset and MMVED-REG on the NUS dataset when analyzing the sensitivity of λ . The most salient one is that for MMVED-TMP, the optimal value for λ shifts to a smaller value 0.3, which implies that under our model design and experimental settings, less constraint leads to better performance for the temporal popularity regression task. Moreover, for MMVED-TMP model, if no constraint is set upon the hidden representation ($\lambda=0$), although over-fits quickly, which is reflected by the rapid rebound of validation loss, the training loss converges for all splits (while for MMVED-REG model, training fails to converge for some splits). Such phenomena could be explained as follows: First, in [12], by visualizing the statistical characteristics of the popularity sequence in a stratified manner, we found that the popularity level of micro-videos tend to have similar temporal evolution patterns, reaching the peak shortly after their launch, and then gradually dropping to near-zero and stabilize, as people show preference to fresh micro-videos than the stale and obsolete ones. Thus, the absolute time which is fed into the RNN at each timestep is itself a strong indicator for popularity level, which makes MMVED-TMP less dependent on the latent representation compared to MMVED-REG, for which, on the contrary, the noisy micro-video content is the sole source of information. Therefore, the MMVED-TMP model exhibits more tolerance to the irrelevant information in the hidden representation. Since empirically, setting λ to 0.3 reaches the optimal performance for the MMVED-TMP model, we use it as the default value for λ in the sections afterwards.

Table 3: Comparison of performance between the proposed MMVED-TMP model and several baseline methods.

Methods	nMSE-TMP	SRC
Temporal SVR	1.018	0.247
Temporal RFR	1.204	0.127
CLSTM	0.987	0.634
MMDED	0.979	0.655
The proposed MMVED-TMP	0.971	0.767

The best results are in bold.

Small nMSE and large SRC indicate good performance.

6.2.3 Comparison with the Baselines

In order to further prove the effectiveness of the proposed MMVED-TMP model, in this section, we choose two machine learning baselines, i.e., the temporal support vector regressor and the temporal random forest, and two deep learning baselines, i.e., the contextual LSTM, the multimodal deterministic encoder-decoder, to verify the superiority of the proposed MMVED-TMP framework:

- **Temporal SVR.** The Support Vector Regressor (SVR) is a widely-used kernel method in regression areas. For SVR to be amenable to the temporal regression task, the absolute time is jointly concatenated with the features of micro-videos from four modalities.
- **Temporal RFR.** The Random Forest Regressor (RFR) is another machine learning method based on an ensemble of decision trees. We make the same pre-processing for features as the Temporal SVR to make the RFR suitable for the temporal prediction task.
- **Contextual LSTM.** The Contextual LSTM [49] augments the input at each timestep of the LSTM with a global embedding of the object as auxiliary contextual information. In our implementation, we encode the concatenation of features from all modalities with an MLP as the contextual variable.
- **Deterministic Encoder-Decoder.** In order to verify the effectiveness of uncertainty preservation, we design the multimodal deterministic encoder-decoder (MMDED) baseline, where the mean of the PoE Gaussian embedding is taken as a deterministic representation of the input modalities. All other structures remain the same as the MMVED-TMP.

Table 3 summarizes the comparison of performance between the proposed MMVED-TMP model and the baselines. Three conclusions can be drawn from the Table 3: First, deep learning-based methods consistently outperform the machine learning-based ones by a large margin, since for the machine learning-based baselines, the prediction of popularity level at each timestep is made independently by taking the absolute time as an auxiliary 1D-feature, and thus no temporal relationship is utilized in these methods, whereas capturing the dynamic pattern of sequence, on the contrary, is the strength of the RNNs. Second, for the encode-decoder based deep learning methods, those that take the hidden encoding as the initial state of the RNN (MMDED, MMVED-TMP) outperform those use hidden encoding to aug-

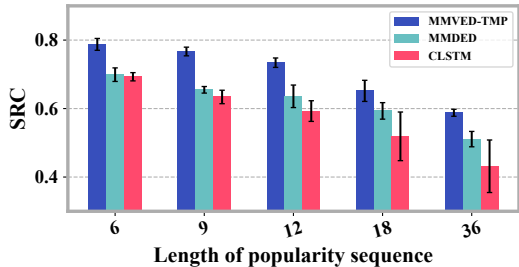


Figure 5: The influence of sampling granularity (sequence length) to performance of proposed MMVED-TMP and two RNN-based baselines

ment the input at each timestep (CLSTM). The reason could be that by only using the embedding micro-video as an initialization for the hidden state of the RNN, the former methods force the encoder to summarize relevant information from the micro-video features with respect to the popularity trend, blocking the undesired shortcut for the network to base the prediction solely on the absolute time and ignore the encoding. Besides, by concatenating the high dimensional micro-video feature with the absolute time, the CLSTM model dilates the 1D absolute time information, which is shown to be the strong indicator for the popularity trend of the micro-videos in the previous section.

Finally, we also confirm that modeling the hidden representation as a stochastic variable (MMVED-TMP) performs better than its deterministic counterpart (MMDED). Two reasons could explain such result: first, the mapping from the feature of micro-video to its popularity trend is non-deterministic as external uncertain factors also influence its popularity level, and encoding the micro-video content into stochastic Gaussian embedding where the uncertainty is preserved in its variance is flexible enough to deal with such randomness. Besides, the MMVED-TMP is able to systematically model the hidden noise generative process by adding a self-adaptive noise to its encoded hidden representation during the training phase, which shows more robustness to noise than the MMDDED model when faced with new data.

6.2.4 Influence of Sampling Granularity

In order to gain more insight into the effects of the popularity sequence length to the performance of the proposed MMVED-TMP model and the baselines, in this section we test the model performance with varied re-sample interval T_{int} (which, as a result, changes the popularity sequence length). As the change of T_{int} alters the groundtruth variance, which invalidates the comparison of nMSE metric, we only use the SRC metric as the performance indicator. The evaluation results are illustrated in Figure 5. Figure 5 shows that generally, for all three models, SRC drops as the sequence length increases, since longer sequence makes it harder to propagate gradient information at the back of the popularity sequence to both the temporal RNN and the multimodal encoder; Besides, the prediction error could accumulate more severely with longer output sequences. However, even for popularity sequence of length 36, which is quite large due to the off-line nature of our task, the prediction made by MMVED-TMP still gets more than 0.5 of correlation with the groundtruth and shows the lowest variance of all dataset splits compared with two other baselines, which demonstrates the

Table 4: Influence of modality missing problems to MMVED-TMP model under nMSE and SRC criteria.

Available Modalities	nMSE-TMP	SRC
A + T + S	0.9706	0.7669
V + T + S	0.9707	0.7670
V + A + S	0.9705	0.7669
V + T + A	0.9710	0.7614
No missing modality	0.9705	0.7667

potential generalization ability of the proposed MMVED-TMP model to popularity prediction tasks with finer granularity and longer term.

6.2.5 Robustness to Modality Missing in Test Phase

Finally, in this section, we demonstrate the robustness of our model under the circumstances where some modalities are missing in the test phase. Such a problem is quite common since some users are naturally reluctant to turn on the microphone when film their videos, to add descriptions to their posted micro-videos, or to upload any user profile. As is mentioned in section 3.3, with the conditional independence assumption, when faced with new samples with fewer modalities than those in the training set, we simply drop the corresponding encoder networks and re-compute the product-of-experts distribution with the encodings calculated from the available modalities, saving the effort to re-train the whole MMVED framework from scratch.

In the experiments, we fix the weights of the trained MMVED-TMP model, eliminate one modality with the corresponding encoder network at a time, and report the test performance. The results are listed in Table 4. From Table 4, we can find out that the detrimental effect of missing one modality is quite negligible. Aside from the strong temporal features, such results could also be explained by the PoE nature of the multimodal encoder, where the decision for which information to encode from the micro-video content into the hidden representation is made based on the complementary information from all modalities, weighted by their confidence. We observe that the elimination of social modality costs the performance the most, which is in agreement with [21], accentuating the important role the uploader plays for the potential popularity of a micro-video. The elimination of visual and aural modality, on the other hand, shows least effects on the performance, since although features from both modalities have the largest dimension, they are redundant and can be complemented by information from other available modalities, whereas the user attributes from the social modality are compact and comparatively irreplaceable.

7 CONCLUSIONS

In this paper, we propose a multimodal variational encoder-decoder (MMVED) framework for micro-video popularity prediction tasks. The proposed MMVED is capable of learning a stochastic Gaussian embedding of a micro-video that is informative to its potential popularity level, where the inherent uncertainty is properly preserved. Besides, faced with the internal noise of micro-videos, a deep information bottleneck constraint is set upon the Gaussian embedding such that only

relevant information is allowed to flow from the input modalities to the hidden representations.

Based on experiments on two real-world datasets, we draw the following conclusions: First, explicitly taking the uncertainty into consideration by modeling the hidden representation as random variables could improve the performance of micro-video popularity prediction models compared with their deterministic counterpart. Second, it is necessary to make constraints on the information contained in the stochastic embedding to deal with the noise in micro-video features, such trained models can achieve satisfactory generalization abilities.

REFERENCES

- [1] Dongliang Liao, Jin Xu, Gongfu Li, Weijie Huang, Weiqing Liu, and Jing Li. Popularity prediction on online articles with deep fusion of temporal process and content features. In *AAAI Conference on Artificial Intelligence*, volume 33, pages 200–207, 2019.
- [2] Jingyuan Chen, Xuemeng Song, Liqiang Nie, Xiang Wang, Hanwang Zhang, and Tat-Seng Chua. Micro tells macro: Predicting the popularity of micro-videos via a transductive model. In *ACM International Conference on Multimedia*, pages 898–907, 2016.
- [3] Ming Zeng, Tzu-Heng Lin, Min Chen, Huan Yan, Jiaxin Huang, Jing Wu, and Yong Li. Temporal-spatial mobile application usage understanding and popularity prediction for edge caching. *IEEE Wireless Communications*, 25(3): 36–42, 2018.
- [4] Adam Bielski and Tomasz Trzcinski. Understanding multimodal popularity prediction of social media videos with self-attention. *IEEE Access*, 6:74277–74287, 2018.
- [5] Kelwin Fernandes, Pedro Vinagre, and Paulo Cortez. A proactive intelligent decision support system for predicting the popularity of online news. In *Portuguese Conference on Artificial Intelligence*, pages 535–546, 2015.
- [6] Philip J McParlane, Yashar Moshfeghi, and Joemon M Jose. Nobody comes here anymore, it’s too crowded; predicting image popularity on Flickr. In *International Conference on Multimedia Retrieval*, page 385, 2014.
- [7] Guandan Chen, Qingchao Kong, Nan Xu, and Wenji Mao. NPP: A neural popularity prediction model for social media content. *Neurocomputing*, 333:221–230, 2019.
- [8] Alexandru Tatar, Jérémie Leguay, Panayotis Antoniadis, Arnaud Limbourg, Marcelo Dias de Amorim, and Serge Fdida. Predicting the popularity of online articles based on user comments. In *International Conference on Web Intelligence, Mining and Semantics*, page 67, 2011.
- [9] Ying Hu, Changjun Hu, Shushen Fu, Peng Shi, and Bowen Ning. Predicting the popularity of viral topics based on time series forecasting. *Neurocomputing*, 210:55–65, 2016.
- [10] Henrique Pinto, Jussara M Almeida, and Marcos A Gonçalves. Using early view patterns to predict the popularity of YouTube videos. In *ACM International Conference on Web Search and Data Mining*, pages 365–374, 2013.
- [11] Shangfei Wang, Can Wang, Tanfang Chen, Yaxin Wang, Yangyang Shu, and Qiang Ji. Video affective content analysis by exploring domain knowledge. *IEEE Transactions on Affective Computing*, 2019.
- [12] Jiayi Xie, Yaochen Zhu, Zhibin Zhang, Jian Peng, Jing Yi, Yaosi Hu, Hongyi Liu, and Zhenzhong Chen. A multi-modal variational encoder-decoder framework for micro-video popularity prediction. In *The World Wide Web Conference*, 2020.
- [13] Shing H Doong. Predicting Twitter hashtags popularity level. In *International Conference on System Sciences*, pages 1959–1968, 2016.
- [14] Zongyang Ma, Aixin Sun, and Gao Cong. On predicting the popularity of newly emerging hashtags in Twitter. *Journal of the American Society for Information Science and Technology*, 64(7):1399–1410, 2013.
- [15] Victoria Zayats and Mari Ostendorf. Conversation modeling on Reddit using a graph-structured LSTM. *Transactions of the Association for Computational Linguistics*, 6: 121–132, 2018.
- [16] Suman Deb Roy, Tao Mei, Wenjun Zeng, and Shipeng Li. Towards cross-domain learning for social video popularity prediction. *IEEE Transactions on multimedia*, 15(6):1255–1267, 2013.
- [17] Haitao Li, Xiaoqiang Ma, Feng Wang, Jiangchuan Liu, and Ke Xu. On popularity prediction of videos shared in online social networks. In *ACM International Conference on Information and Knowledge Management*, pages 169–178, 2013.
- [18] Aditya Khosla, Atish Das Sarma, and Raffay Hamid. What makes an image popular? In *International Conference on World Wide Web*, pages 867–876, 2014.
- [19] Qi Cao, Huawei Shen, Jinhua Gao, Bingzheng Wei, and Xueqi Cheng. Popularity prediction on social platforms with coupled graph neural networks. In *International Conference on Web Search and Data Mining*, pages 70–78, 2020.
- [20] Tomasz Trzciński and Przemysław Rokita. Predicting popularity of online videos using support vector regression. *IEEE Transactions on Multimedia*, 19(11):2561–2570, 2017.
- [21] Peiguang Jing, Yuting Su, Liqiang Nie, Xu Bai, Jing Liu, and Meng Wang. Low-rank multi-view embedding learning for micro-video popularity prediction. *IEEE Transactions on Knowledge and Data Engineering*, 30(8):1519–1532, 2017.
- [22] Naftali Tishby, Fernando C. Pereira, and William Bialek. The information bottleneck method. In *Annual Allerton Conference on Communication, Control and Computing*, pages 368–377, 1999.
- [23] David M Blei, Alp Kucukelbir, and Jon D McAuliffe. Variational inference: A review for statisticians. *Journal of the American Statistical Association*, 112(518):859–877, 2017.
- [24] Cees GM Snoek, Marcel Worring, and Arnold WM Smeulders. Early versus late fusion in semantic video analysis.

- In *ACM International Conference on Multimedia*, pages 399–402, 2005.
- [25] Mike Wu and Noah Goodman. Multimodal generative models for scalable weakly-supervised learning. In *Advances in Neural Information Processing Systems*, pages 5580–5590, 2018.
- [26] Yaochen Zhu, Zhenzhong Chen, and Feng Wu. Multimodal deep denoise framework for affective video content analysis. In *ACM International Conference on Multimedia*, pages 130–138, 2019.
- [27] Geoffrey E Hinton. Training products of experts by minimizing contrastive divergence. *Neural Computation*, 14(8):1771–1800, 2002.
- [28] Sepp Hochreiter and Jürgen Schmidhuber. Long short-term memory. *Neural Computation*, 9(8):1735–1780, 1997.
- [29] Marc’Aurelio Ranzato, Sumit Chopra, Michael Auli, and Wojciech Zaremba. Sequence level training with recurrent neural networks. *arXiv preprint arXiv:1511.06732*, 2015.
- [30] Yoshua Bengio, Réjean Ducharme, Pascal Vincent, and Christian Jauvin. A neural probabilistic language model. *Journal of Machine Learning Research*, 3(Feb):1137–1155, 2003.
- [31] Diederik P Kingma and Max Welling. Auto-encoding variational Bayes. *arXiv preprint arXiv:1312.6114*, 2013.
- [32] Yarín Gal. *Uncertainty in deep learning*. PhD thesis, University of Cambridge, 2016.
- [33] Xiaopeng Li and James She. Collaborative variational autoencoder for recommender systems. In *ACM International Conference on Knowledge Discovery and Data Mining*, pages 305–314, 2017.
- [34] Kaiming He, Xiangyu Zhang, Shaoqing Ren, and Jian Sun. Deep residual learning for image recognition. In *IEEE Conference on Computer Vision and Pattern Recognition*, pages 770–778, 2016.
- [35] Olga Russakovsky, Jia Deng, Hao Su, Jonathan Krause, Sanjeev Satheesh, Sean Ma, Zhiheng Huang, Andrej Karpathy, Aditya Khosla, Michael Bernstein, et al. ImageNet large scale visual recognition challenge. *International Journal of Computer Vision*, 115(3):211–252, 2015.
- [36] Matthew D Zeiler and Rob Fergus. Visualizing and understanding convolutional networks. In *European Conference on Computer Vision*, pages 818–833, 2014.
- [37] Yinwei Wei, Xiang Wang, Liqiang Nie, Xiangnan He, Richang Hong, and Tat-Seng Chua. MMGCN: Multimodal graph convolution network for personalized recommendation of micro-video. In *ACM International Conference on Multimedia*, pages 1437–1445, 2019.
- [38] Yinwei Wei, Zhiyong Cheng, Xuzheng Yu, Zhou Zhao, Lei Zhu, and Liqiang Nie. Personalized hashtag recommendation for micro-videos. In *ACM International Conference on Multimedia*, pages 1446–1454, 2019.
- [39] Shawn Hershey, Sourish Chaudhuri, Daniel PW Ellis, Jort F Gemmeke, Aren Jansen, R Channing Moore, Manoj Plakal, Devin Platt, Rif A Saurous, Bryan Seybold, et al. CNN architectures for large-scale audio classification. In *IEEE International Conference on Acoustics, Speech and Signal Processing*, pages 131–135, 2017.
- [40] Jort F Gemmeke, Daniel PW Ellis, Dylan Freedman, Aren Jansen, Wade Lawrence, R Channing Moore, Manoj Plakal, and Marvin Ritter. Audio Set: An ontology and human-labeled dataset for audio events. In *IEEE International Conference on Acoustics, Speech and Signal Processing*, pages 776–780. IEEE, 2017.
- [41] Xipeng Qiu, Qi Zhang, and Xuanjing Huang. FudanNLP: A toolkit for Chinese natural language processing. In *Annual Meeting of the Association for Computational Linguistics: System Demonstrations*, pages 49–54, 2013.
- [42] Quoc Le and Tomas Mikolov. Distributed representations of sentences and documents. In *International Conference on Machine Learning*, pages 1188–1196, 2014.
- [43] Christopher D. Manning, Mihai Surdeanu, John Bauer, Jenny Finkel, Steven J. Bethard, and David McClosky. The Stanford CoreNLP natural language processing toolkit. In *Association for Computational Linguistics System Demonstrations*, pages 55–60, 2014.
- [44] Richard Socher, Alex Perelygin, Jean Wu, Jason Chuang, Christopher D Manning, Andrew Y Ng, and Christopher Potts. Recursive deep models for semantic compositionality over a sentiment treebank. In *The Conference on Empirical Methods in Natural Language Processing*, pages 1631–1642, 2013.
- [45] Diederik P. Kingma and Jimmy Ba. Adam: A method for stochastic optimization. In *International Conference on Learning Representations*, 2015.
- [46] Liqiang Nie, Luming Zhang, Yi Yang, Meng Wang, Richang Hong, and Tat-Seng Chua. Beyond doctors: Future health prediction from multimedia and multimodal observations. In *ACM international conference on Multimedia*, pages 591–600, 2015.
- [47] Guang-Bin Huang, Qin-Yu Zhu, and Chee-Kheong Siew. Extreme learning machine: Theory and applications. *Neurocomputing*, 70(1-3):489–501, 2006.
- [48] Guang-Bin Huang, Hongming Zhou, Xiaojuan Ding, and Rui Zhang. Extreme learning machine for regression and multiclass classification. *IEEE Transactions on Systems, Man, and Cybernetics, Part B*, 42(2):513–529, 2011.
- [49] Shalini Ghosh, Oriol Vinyals, Brian Strope, Scott Roy, Tom Dean, and Larry Heck. Contextual LSTM (CLSTM) models for large scale NLP tasks. *arXiv preprint arXiv:1602.06291*, 2016.

Appendices

A THE DEEP VARIATIONAL INFORMATION BOTTLENECK LOWER BOUND FOR MMVED

Theorem 1. *If $p(\mathbf{z}|\mathbf{m}, \mathbf{y}) = p(\mathbf{z}|\mathbf{m})$ holds, i.e. \mathbf{m} contains all necessary information w.r.t the hidden representation \mathbf{z} , the following information bottleneck inequality holds:*

$$\mathbf{MI}(\mathbf{z}, \mathbf{y}) - \lambda \cdot \mathbf{MI}(\mathbf{z}, \mathbf{m}) \geq \text{IBLBO} \triangleq \mathbb{E}_{p(\mathbf{m}, \mathbf{y})} \left[\mathbb{E}_{p(\mathbf{z}|\mathbf{m})} [\log q(\mathbf{y}|\mathbf{z})] - \lambda \cdot \mathbf{KL}(p(\mathbf{z}|\mathbf{m})||p(\mathbf{z})) \right] \quad (22)$$

where $p(\mathbf{m}, \mathbf{y})$ is the data distribution, $p(\mathbf{z}|\mathbf{m})$ is the encoder distribution, $q(\mathbf{y}|\mathbf{z})$ is the variational decoder distribution and $p(\mathbf{z})$ is the specified prior for \mathbf{z} . In order to prove the theorem, we first prove two lemmas below.

Lemma 2. *Under the assumptions of Theorem 1, the following holds:*

$$\mathbf{MI}(\mathbf{z}, \mathbf{y}) \geq \mathbb{E}_{p(\mathbf{m}, \mathbf{y})} \left[\mathbb{E}_{p(\mathbf{z}|\mathbf{m})} [\log q(\mathbf{y}|\mathbf{z})] \right] \quad (23)$$

Proof. According to the definition of mutual information:

$$\mathbf{MI}(\mathbf{z}, \mathbf{y}) = \mathbb{E}_{p(\mathbf{y}, \mathbf{z})} \left[\log \frac{p(\mathbf{y}, \mathbf{z})}{p(\mathbf{y})p(\mathbf{z})} \right] = \mathbb{E}_{p(\mathbf{y}, \mathbf{z})} \left[\log \frac{p(\mathbf{y}|\mathbf{z})}{p(\mathbf{y})} \right] \quad (24)$$

Observing that the KL-divergence is non-negative, the following inequality holds.

$$\mathbf{KL}[p(\mathbf{y}|\mathbf{z})||q(\mathbf{y}|\mathbf{z})] \geq 0 \implies \mathbb{E}_{p(\mathbf{y}|\mathbf{z})} [\log p(\mathbf{y}|\mathbf{z})] \geq \mathbb{E}_{p(\mathbf{y}|\mathbf{z})} [\log q(\mathbf{y}|\mathbf{z})] \quad (25)$$

Then, the $\mathbf{MI}(\mathbf{z}, \mathbf{y})$ is lower-bounded by:

$$\begin{aligned} \mathbf{MI}(\mathbf{z}, \mathbf{y}) &\geq \mathbb{E}_{p(\mathbf{y}, \mathbf{z})} \left[\log \frac{p(\mathbf{y}|\mathbf{z})}{p(\mathbf{y})} \right] \\ &= \mathbb{E}_{p(\mathbf{y}, \mathbf{z})} \log q(\mathbf{y}|\mathbf{z}) - \mathbb{E}_{p(\mathbf{y})} \log p(\mathbf{y}) \\ &= \mathbb{E}_{p(\mathbf{y}, \mathbf{z})} \log q(\mathbf{y}|\mathbf{z}) + \mathbf{H}(\mathbf{y}) \end{aligned} \quad (26)$$

Since $\mathbf{H}(\mathbf{y})$ is the entropy of \mathbf{y} , which is a positive constant independent of the hidden encoding \mathbf{z} , it can be safely ignored. According to the independence assumption of Theorem 1, $p(\mathbf{y}, \mathbf{z}) = \int p(\mathbf{m}, \mathbf{y}, \mathbf{z}) d\mathbf{m} = \int p(\mathbf{m})p(\mathbf{y}|\mathbf{m})p(\mathbf{z}|\mathbf{m})d\mathbf{m}$, then, a new lower bound of $\mathbf{MI}(\mathbf{z}, \mathbf{y})$ can be deduced:

$$\begin{aligned} \mathbf{MI}(\mathbf{z}, \mathbf{y}) &\geq \int p(\mathbf{m})p(\mathbf{y}|\mathbf{m})p(\mathbf{z}|\mathbf{m}) \log q(\mathbf{y}|\mathbf{z}) d\mathbf{m} d\mathbf{y} d\mathbf{z} \\ &= \mathbb{E}_{p(\mathbf{m}, \mathbf{y})} \left[\mathbb{E}_{p(\mathbf{z}|\mathbf{m})} [\log q(\mathbf{y}|\mathbf{z})] \right] \end{aligned} \quad (27)$$

which finishes our proof of Lemma 2. \square

Lemma 3. *Under the assumptions of Theorem 1, the following holds:*

$$\mathbf{MI}(\mathbf{z}, \mathbf{m}) \leq \mathbb{E}_{p(\mathbf{m}, \mathbf{y})} [\mathbf{KL}[p(\mathbf{z}|\mathbf{m})||p(\mathbf{z})]] \quad (28)_{14}$$

Proof. For clarity, with a little misuse of notation, we use $\hat{p}(\mathbf{z})$ to denote the marginal distribution and $p(\mathbf{z})$ as the assumed prior. Observing the fact that

$$\mathbf{KL}[\hat{p}(\mathbf{z})||q(\mathbf{z})] \geq 0 \implies \mathbb{E}_{\hat{p}(\mathbf{z})} [\log \hat{p}(\mathbf{z})] \geq \mathbb{E}_{\hat{p}(\mathbf{z})} [\log q(\mathbf{z})] \quad (29)$$

The following upper bound can be obtained:

$$\begin{aligned} \mathbf{MI}(\mathbf{z}, \mathbf{m}) &\leq \int p(\mathbf{m})p(\mathbf{z}|\mathbf{m}) \log \frac{p(\mathbf{z}|\mathbf{m})}{p(\mathbf{z})} d\mathbf{m} d\mathbf{z} \\ &= \int p(\mathbf{m})p(\mathbf{y}|\mathbf{m})p(\mathbf{z}|\mathbf{m}) \log \frac{p(\mathbf{z}|\mathbf{m})}{p(\mathbf{z})} d\mathbf{y} d\mathbf{m} d\mathbf{z} \\ &= \mathbb{E}_{p(\mathbf{m}, \mathbf{y})} [\mathbf{KL}[p(\mathbf{z}|\mathbf{m})||p(\mathbf{z})]] \end{aligned} \quad (30)$$

which finishes our proof of Lemma 3. \square

Finally, combining the two bounds of Lemma 2 and 3 finishes the proof for Theorem 1.

B MULTIMODAL PRODUCT-OF-EXPERTS ENCODER WITH CONDITIONAL INDEPENDENCE ASSUMPTION

By making the conditional independence assumption, i.e., assuming $(\mathbf{m}_i \perp \mathbf{m}_j|\mathbf{z}) \quad \forall i, j < K$ and $i \neq j$ and using the Bayesian rule, the following equation holds:

$$\begin{aligned} p(\mathbf{z}|\mathbf{m}) &= \frac{p(\mathbf{m}|\mathbf{z})p(\mathbf{z})}{p(\mathbf{m})} = \frac{p(\mathbf{z})}{p(\mathbf{m})} \prod_{i=1}^K p(\mathbf{m}_i|\mathbf{z}) \\ &= \frac{p(\mathbf{z})}{p(\mathbf{m})} \prod_{i=1}^K \frac{p(\mathbf{z}|\mathbf{m}_i)p(\mathbf{m}_i)}{p(\mathbf{z})} \propto \frac{\prod_{i=1}^K p(\mathbf{z}|\mathbf{m}_i)}{\prod_{i=1}^{K-1} p(\mathbf{z})} \end{aligned} \quad (31)$$

Moreover, to avoid quotient of probability distributions, we further assume that $p(\mathbf{z}|\mathbf{m}_i)$ can be approximated with $\tilde{p}(\mathbf{z}|\mathbf{m}_i)p(\mathbf{z})$, where $\tilde{p}(\mathbf{z}|\mathbf{m}_i)$ is the encoder network for the i th modality, and $p(\mathbf{z})$ is the prior. Then, the following simplification of Eq. 31 can be made:

$$\begin{aligned} p(\mathbf{z}|\mathbf{m}) &\propto \frac{\prod_{i=1}^K p(\mathbf{z}|\mathbf{m}_i)}{\prod_{i=1}^{K-1} p(\mathbf{z})} \approx \\ &= \frac{\prod_{i=1}^K [\tilde{p}(\mathbf{z}|\mathbf{m}_i)p(\mathbf{z})]}{\prod_{i=1}^{K-1} p(\mathbf{z})} = p(\mathbf{z}) \prod_{i=1}^K \tilde{p}(\mathbf{z}|\mathbf{m}_i) \end{aligned} \quad (32)$$

which finishes the deduction for the product-of-experts based multimodal encoder utilized in our paper.